2013

Spatio-temporal Patterns of Pre-harvest Brown Rot Epidemics within Individual Peach Tree Canopies

Sydney E. Everhart
University of Georgia, everhart@unl.edu

A. Askew
University of Georgia, Athens

L. Seymour
University of Georgia, Athens

H. Scherm
University of Georgia, Athens, scherm@uga.edu

Published in *European Journal of Plant Pathology* 135 (2013), pp. 499–508;
doi: 10.1007/s10658-012-0113-3

Accepted October 8, 2012; published online October 24, 2012.

Spatio-temporal Patterns of Pre-harvest Brown Rot Epidemics within Individual Peach Tree Canopies

S. E. Everhart,[1] A. Askew,[2] L. Seymour,[2] H. Scherm[1]

1. Department of Plant Pathology, University of Georgia, Athens, GA 30602, USA
2. Department of Statistics, University of Georgia, Athens, GA 30602, USA

Corresponding author – H. Scherm, email scherm@uga.edu

Abstract
Tree canopies are architecturally complex and pose several challenges for measuring and characterizing spatial patterns of disease. Recently developed methods for fine-scale canopy mapping and three-dimensional spatial pattern analysis were applied in a 3-year study to characterize spatio-temporal development of pre-harvest brown rot of peach, caused by *Monilinia fructicola*, in 13 trees of different maturity classes. We observed a negative correlation between an index of disease aggregation and disease incidence in the same tree ($r = -0.653$, $P < 0.0001$), showing that trees with higher brown rot incidence had lower aggregation of affected fruit in their canopies. Significant ($P \leq 0.05$) within-canopy aggregation among symptomatic fruit was most pronounced for early-maturing cultivars and/or early in the epidemic. This is consistent with the notion of a greater importance of localized, within-tree sources of inoculum at the beginning of the epidemic. Four of five trees having >10 blossom blight symptoms per tree showed a significant positive spatial association of pre-harvest fruit rot to blossom blight within the same canopy. Spatial association analyses further revealed one of two outcomes for the association of new fruit rot symptoms with previous fruit rot symptoms in the same tree, whereby the relationship was either not significant or exhibited a significant negative association. In the latter scenario, the newly diseased fruit were farther apart from previously symptomatic fruit than expected by random chance. This unexpected result could have been due to uneven fruit ripening in different sectors of the canopy, which could have affected the timing of symptom development and thus led to negative spatial associations among symptoms developing over time in a tree.

Keywords: canopy, *Monilinia fructicola*, peach, *Prunus persica*, spatial analysis, spatial pattern

Introduction

Analysis of spatial patterns of plant disease as a means of quantifying spatial structure and inferring processes has come of age during the past two decades (Jeger 1999; Madden et al. 2007; Waggoner and Aylor 2000). In recent years, emphasis has begun to broaden from the traditional focus of characterizing disease patterns at the field scale toward analyzing spatial patterns at larger (landscape) or smaller (within-plant) scales, or across hierarchies from plants to landscapes (Moslonka-Lefebvre et al. 2010; Plantegenest et al. 2007; Vereijssen et al. 2007). Nevertheless, there is a paucity of research addressing plant disease aggregation and association patterns in individual plant canopies, especially in trees which possess complex canopies. Such within-canopy patterns may arise due to the nonrandom arrangement of susceptible plant parts (such as fruit, blossoms, or leaves) in the tree canopy, and/or the proximity of within-tree inoculum sources (such as cankers). Disease patterns in tree canopies may also be influenced by abiotic factors such as within-tree variability in microclimate (e.g., wetness duration) or fungicide coverage (Batzer et al. 2008; Smith and MacHardy 1984). Thus, pathogen, host, and abiotic factors may interact to produce complex spatial patterns of disease within these canopies.

Characterization of spatial patterns of disease in tree canopies is challenged by difficulty in recording spatial location of symptomatic tissues and in selecting the appropriate statistical approach that will account for the naturally nonrandom pattern of susceptible plant parts. Previous studies examining spatial disease patterns within tree canopies either divided the canopy into layers (Holb and Scherm 2007) or quadrats (Batzer et al. 2008; Spósito et al. 2008). However, an important limitation of using such stratification is that the associated grouping of data may fail to capture fine-scale patterns within each block. In a recent pilot study (Everhart et al. 2011) we used a magnetic digitizer to map different brown rot symptom types (blossom blight, shoot blight, and twig cankers) caused by the fungal plant pathogen *Monilinia laxa* in individual sour cherry canopies and applied nearest-neighbor-based spatial analysis methods to the resultant three-dimensional map of data points. This enabled us to determine the level of aggregation of different symptom types in the canopy as well as the degree of association of current year's symptoms with symptoms from the previous year's infections. However, since disease assessment and mapping in the aforementioned study were done at a single point in time, prior to the period of fruit maturation, it was not possible to analyze spatio-temporal disease development or to quantify spatial patterns of pre-harvest fruit rot, the most important symptom type, within the canopy. Hence, we designed a 3-year follow-up study on peach (*Prunus persica*) to monitor the spatio-temporal development of brown rot (caused by *Monilinia fructicola*) during the course of the season and to quantify spatial aggregation and association patterns within each canopy. Preliminary results based on the first year of data have been reported in a conference paper (Everhart et al. 2012).

Materials and methods

Disease monitoring and canopy mapping

The study was conducted in an experimental peach orchard at the University of Georgia Horticulture Farm (Watkinsville, Georgia, USA) from late March to September in 2009, 2010, and 2011. The orchard had been planted in 2000 and consisted of six cultivars of varying maturity classes, arranged in replicate four-tree plots having within and across-row spacing of 4.6 and 6.1 m, respectively. Early-season cultivars attained commercial ripeness in mid-June, mid-season cultivars in early July, and late-season cultivars in early August. No fungicide applications to control brown rot were made to the test trees, but foliar sprays of wettable sulphur were applied during the cover spray period across the orchard to suppress peach scab (caused by *Fusicladium carpophilum*). All other horticultural and pest management followed standard commercial practice (Horton et al. 2011). Trees were thinned relatively lightly to ensure a sufficient number of fruit per tree for within-tree mapping and spatial analysis.

Factors considered in selection of the individual trees used in this study were as follows: canopy shape and architecture (spherical to oblong, without major gaps); size of the tree (characteristic size of 1.3 to 2.0 m high and 2.9 to 5.8 m wide); and inclusion of trees from early-, mid-, and late-season maturity classes. Some trees were monitored for disease from blossom blight to fruit drop, whereas others were monitored only during the pre-harvest fruit rot phase. Candidate trees were selected in the spring based on the aforementioned criteria. As the season progressed, some trees were eliminated from the monitoring based on factors such as lack of disease development, limb breakage, and bird or insect damage to fruit. Collectively across the 3 years, this process resulted in a final set of 13 trees of different maturity classes and varying levels of disease incidence at the end of the season (table 1).

Table 1. Spatial aggregation patterns of pre-harvest brown rot, caused by *Monilinia fructicola*, in 13 intensively mapped peach tree canopies

Cultivar and tree number[a]	Year	Total fruit	Assessment period[b]	Symptomatic fruit	Disease incid. (%)	d_w[c]	*P*	Pattern
Early-season cultivar								
Sureprince 79	2010	250	Early	26	10.4	**0.375**	0.004	Aggregated
			Mid	48	19.2	**0.291**	0.004	Aggregated
			Late	83	33.2	**0.177**	0.015	Aggregated

Mid-season cultivars								
Redglobe 7	2009	248	Early	26	10.5	0.135	0.812	Random
			Mid	63	25.4	0.116	0.454	Random
			Late	87	35.1	0.099	0.405	Random
Contender 74	2010	433	Early	41	9.5	**0.240**	0.042	Aggregated
			Late	123	28.4	0.123	0.075	Random
Contender 75	2010	392	Early	12	3.1	**0.616**	0.000	Aggregated
			Mid	48	12.2	**0.254**	0.018	Aggregated
			Late	59	15.1	0.179	0.103	Random
Late-season cultivars								
O'Henry 26	2009	244	Early	35	14.3	**0.360**	0.003	Aggregated
			Mid	128	52.5	0.079	0.342	Random
			Late	142	58.2	0.047	0.806	Random
O'Henry 26	2010	486	Early	18	3.7	**0.440**	0.010	Aggregated
			Mid	67	13.8	**0.330**	0.000	Aggregated
			Late	88	18.1	**0.290**	0.000	Aggregated
O'Henry 26	2011	861	Early	21	2.4	0.226	0.310	Random
			Mid	56	6.5	**0.290**	0.031	Aggregated
			Late	96	11.1	0.104	0.363	Random
O'Henry 127	2009	126	Early	25	19.8	**0.359**	0.024	Aggregated
			Late	38	30.2	**0.264**	0.026	Aggregated
Flameprince 45	2009	385	Early	122	31.7	−0.116	0.097	Random
			Late	169	43.9	−0.064	0.450	Random
Flameprince 45	2010	739	GFR	10	1.4	**0.408**	0.049	Aggregated
			Early	74	10.0	**0.193**	0.034	Aggregated
			Mid	133	18.0	**0.203**	0.000	Aggregated
			Late	155	21.0	**0.216**	0.000	Aggregated
Flameprince 87	2010	601	Early	31	5.2	0.263	0.079	Random
			Mid	61	10.1	**0.218**	0.023	Aggregated
			Late	74	12.3	**0.186**	0.036	Aggregated

Flameprince 88	2010	369	Early	30	7.6	0.223	0.213	Random
			Mid	46	11.6	0.201	0.107	Random
			Late	62	15.7	0.146	0.237	Random
Flameprince 120	2009	396	Early	76	19.2	0.128	0.256	Random
			Late	128	32.3	0.054	0.821	Random

a. Arranged in order of earliest to latest-maturing cultivar.

b. Trees were monitored for disease at 1- to 4-day intervals during the pre-harvest period, and data are summarized for two, three, or four assessment periods for each tree to facilitate data presentation and analysis. In Flameprince 45 (2010), GFR represents fruit affected by green fruit rot that directly preceded the pre-harvest epidemic.

c. d_w represents the index of disease aggregation and is calculated based on the cumulative frequency distribution of nearest-neighbor distances among brown rot–affected fruit. Significant positive values indicate aggregation, whereas significant negative values correspond to a more regular distribution compared with the random simulation. Significant d_w values ($P \leq 0.05$) are in bold.

Trees were observed for disease at 3- to 5-day intervals through final fruit swell and then every 1 to 4 days until fruit were tree-ripe. Symptoms and signs associated with *M. fructicola* infections, including blossom blight, twig blight, twig cankers, green fruit rot, and brown rot of mature fruit were noted, and the position of each was preserved by tying a plastic label on the twig proximal to the node associated with the symptom. Each label was marked with the date of symptom appearance and a unique identifying number. Thus, the spatial location and approximate date of appearance of each symptom were preserved.

In six of the 13 trees, *M. fructicola* was recovered from each symptom at the time of symptom appearance to determine the fine-scale genetic structure of the pathogen within and across canopies (Everhart 2012). The methods for pathogen isolation and genotyping as well as the results and interpretation of the population genetic analyses are beyond the scope of this paper and will be reported elsewhere.

High-resolution three-dimensional maps of the positions of symptom tags and of all fruit (symptomatic and asymptomatic) were created for each tree using a magnetic digitizer (FASTRAK 3Space, Polhemus, Colchester, Vermont, USA; Sinoquet et al. 1997). This device creates a low-level electromagnetic field from an emitter positioned at the base of the tree and allows the user to position a sensor at the location of each point and record the corresponding *x*-, *y*-, and *z*-coordinates (Everhart et al. 2011). The instrument's range and accuracy are 4.6 m and 0.76 mm, respectively. Trees were digitized once in 2009 (when fruit were tree-ripe) and twice in 2010 and 2011 (at the beginning of the pre-harvest interval for all fruit and again at the end of the epidemic for all tagged symptoms). The resultant data set consisted of the *x*-, *y*-, and *z*-coordinates of all fruit (126 to 861) and all symptoms (38 to 169) for each tree, along with the date when each symptom was first recorded.

Analysis of spatial aggregation and association

Spatial patterns of aggregation of fruit affected by brown rot within the canopy were characterized based on the frequency distribution of nearest-neighbor distances among symptomatic fruit in each tree (Everhart et al. 2011). To obtain a corresponding random distribution of the same number of symptoms for comparison, the measured coordinates of all fruit (symptomatic + asymptomatic) were used as a set of coordinates over which the

symptomatic fruit were randomized to generate 1,000 Monte-Carlo simulations for each tree. The cumulative frequency distribution of the observed nearest-neighbor distances among affected fruit was compared with that of the simulations using a Kolmogorov-Smirnov test ($P \leq 0.05$). The test statistic d_w, the maximum departure of the observed cumulative frequency distribution from that of the simulations, was used as an index of spatial aggregation (Coomes et al. 1999). A significant positive value of d_w indicates aggregation, whereas a significant negative value signifies uniformity or regularity. Cumulative frequency distributions of nearest-neighbor distances and the resultant d_w values were used to assess the magnitude and significance of deviation from randomness. All calculations were carried out in Matlab R2011b (Mathworks, Natick, Massachusetts, USA).

Aggregation indexes were calculated separately for different phases (early, mid-period, and late) of the pre-harvest brown rot epidemic (table 1). Each of these phases was defined individually for each tree using roughly equally sized groups of fruit that had become symptomatic over time, or by using natural breakpoints in disease progression. For example, epidemics in which the disease developed gradually were divided into two to three roughly equal-sized groups, with no group containing less than 10 affected fruit. Other epidemics yielded a large number of newly symptomatic fruit in a single assessment, and in those cases symptoms that appeared on the same assessment date were not partitioned into separate groups for analysis.

Nearest-neighbor distances were also used to quantify spatial associations among all pre-harvest fruit rot symptoms to the position of blighted blossoms earlier in the season for trees having 10 or more blossom blight symptoms present (this was the case for five of the 13 trees). Associations among symptomatic fruit within the pre-harvest fruit rot epidemic were similarly compared for all 13 trees between phases of the epidemic recorded at different periods during the pre-harvest interval. A spatial association index was calculated among the fruit that became newly symptomatic during the mid-period (or late period) and those that had been symptomatic in the previous period. As with aggregation, the index of association was based on a comparison of the cumulative frequency distribution of the actual nearest-neighbor distances among fruit in the two classes with that of the corresponding random simulation. In the case of blossom blight association analyses, the randomization consisted of 1,000 Monte-Carlo simulations of pre-harvest fruit rot assigned across the coordinates of all fruit (symptomatic + asymptomatic). In contrast, blossom blight locations maintained a fixed position throughout the simulations. For analysis of spatial associations within the pre-harvest fruit rot epidemic, both the newly affected fruit and the previously affected fruit were randomly assigned across the measured coordinates of all fruit (symptomatic + asymptomatic) in the respective tree. In both cases, the cumulative frequency distributions of the observed and simulated nearest-neighbor distances were compared by Kolmogorov-Smirnov test, and d_w, the maximum departure of the two distributions, was used as an index of association. A significant positive value of d_w indicates positive spatial association (i.e., newly affected and previously affected fruit are located closer to each other than by random chance), whereas a significant negative value signifies negative spatial association.

Results and discussion

Pre-harvest fruit rot epidemics were monitored and mapped in a total of 13 tree canopies across the 3 years, five in 2009, seven in 2010, and one in 2011 (table 1). Disease development was limited in 2011 due to dry weather during the spring and summer, hence only one tree was included from that year; this tree, O'Henry 26, was monitored in all 3 years of the study. Across the 13 trees, the total number of fruit per tree ranged from 126 to 861 (a function of tree size and fruit set in a given year) and final disease incidence at the tree-ripe stage of fruit development from 11.1 to 58.2%.

Median nearest-neighbor distances among all fruit (symptomatic + asymptomatic) varied from 4.5 to 16.9 cm (average: 6.9 cm) across the 13 tree canopies (fig. 1a) and, as expected based on the laws of geometry, correlated negatively with fruit number per tree ($r = -0.595$, $P = 0.032$). For symptomatic fruit at the end of the assessment period, median nearest-neighbor distances were in the range of 10.7 to 20.6 cm with an average of 15.2 cm (fig. 1b). Disease incidence correlated negatively with the number of fruit per tree ($r = -0.613$, $P = 0.026$).

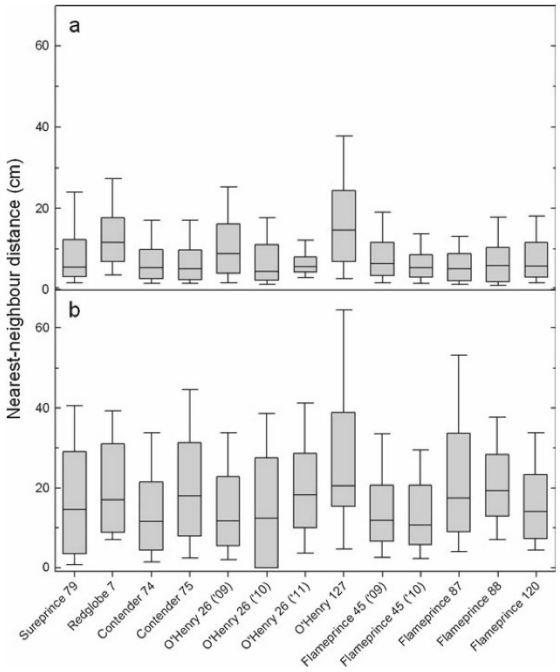

Figure 1. Distribution of nearest-neighbor distances among all fruit (a) and among brown rot–affected fruit at the end of the epidemic (b) in 13 intensively mapped peach tree canopies. Vertical axis labels correspond to cultivar names (arranged in the order of earliest to latest maturity), tree number, and year (in cases where the same tree was monitored in multiple years).

The spatial pattern of pre-harvest fruit rot within individual canopies was assessed at successive intervals (early, mid-period, and late) during the epidemic. Correlation analysis using data from all trees and all intervals revealed a negative relationship between the index of aggregation and disease incidence (fig. 2; $r = -0.653$, $P < 0.0001$). Thus, trees with higher brown rot incidence had lower aggregation of affected fruit within their canopies. Decreasing spatial structure with increasing disease incidence is also commonly observed in studies reporting two-dimensional spatial analyses, e.g., among plants within a field (Pethybridge et al. 2010; Vereijssen et al. 2006). In the present study, there was no correlation between the index of disease aggregation and the total number of fruit per tree ($P = 0.321$).

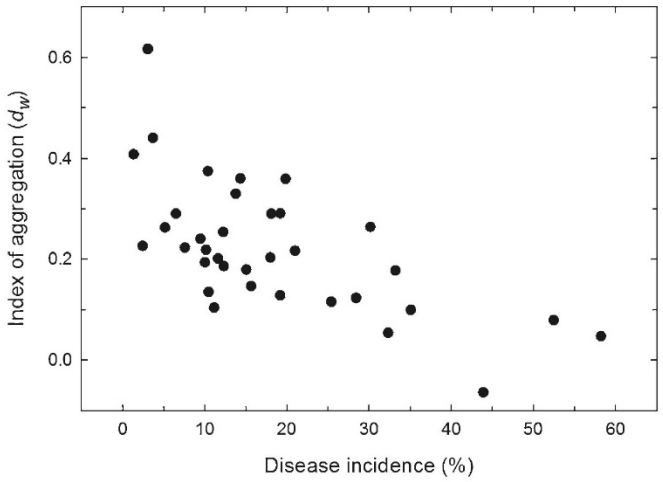

Figure 2. Relationship between spatial aggregation of brown rot–affected fruit and brown rot incidence in 13 intensively mapped peach tree canopies. The two variables correlated significantly ($r = -0.653$, $P < 0.0001$) The index of aggregation d_w is calculated based on the cumulative frequency distribution of nearest-neighbor distances among brown rot–affected fruit. Positive values indicate aggregation, whereas negative values correspond to a more regular distribution compared with the random simulation. Data are from early, mid, and late assessment periods during the epidemic as shown in table 1.

Nine of the 13 trees showed significant within-canopy aggregation of disease for at least one phase of the epidemic, with the remaining four exhibiting random patterns during all phases (table 1). Three of the four trees with consistently random pattern were of the late-season cultivar Flameprince. In these trees, the lack of spatial structure among brown rot–infected fruit could have been due to a dominance of external sources of inoculum in the orchard late in the season owing to the presence of high levels of brown rot in the surrounding early- and mid-season cultivars. For example, the earlier-maturing Contender and Redglobe harbored numerous diseased fruit with abundant *M. fructicola* sporulation in the tree and/or on the ground, while Flameprince was nearing commercial harvest maturity. The fourth tree with a consistently random pattern of pre-harvest brown rot in the canopy was Redglobe 7, a mid-season cultivar that differed from the other trees in that it suffered above-average (>25 %) bird damage to the fruit owing to its location near the edge

of the orchard and being the first to ripen among trees of the same cultivar. Since wounds can serve as important points of entry for *M. fructicola* (Kable 1969), the spatial pattern of wounding and disease may have been confounded in this tree.

All of the early- and mid-season cultivars (with the exception of the aforementioned Redglobe 7) showed an aggregated within-canopy pattern of fruit rot at the early phase of the epidemic. This is consistent with the notion of a greater importance of localized, within-tree sources of inoculum at the beginning of the epidemic in the orchard. Indeed, the earliest-maturing tree, Sureprince 79, exhibited disease aggregation throughout its entire epidemic. In contrast, late-season cultivars showed a lower prevalence of trees with aggregation in the early phase of the epidemic (four of nine trees). Furthermore, regardless of cultivar maturity class, aggregation was less common in the late phase of the epidemic (only five of 13 trees showed significant aggregation), whereby trees with aggregation in the late phase of the epidemic also had aggregation of disease in the early or mid-phase of the epidemic.

Thus, both cultivar maturity season and within-tree epidemic phase (early, mid-period, and late) affected the aggregation pattern of brown rot within canopies, with aggregation being most pronounced for early-season cultivars and/or early in the epidemic for a given tree. In contrast, aggregation was least pronounced in late-season cultivars and/or late into the within-tree epidemic, most likely due to increased inoculum loads in the orchard and in individual trees leading to a more random pattern of disease. A conceptual model linking time, cultivar maturity season, epidemic phase, disease incidence, and disease aggregation based on the relationships observed in this study is depicted in figure 3.

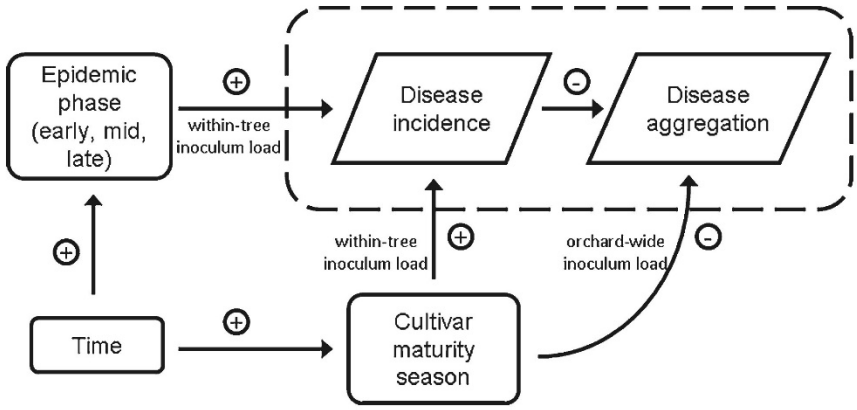

Figure 3. Conceptual model linking time, cultivar maturity season, within-tree epidemic phase, brown rot incidence, and spatial aggregation of brown rot-affected fruit in peach tree canopies. Disease aggregation and disease incidence are correlated negatively (fig. 2). The influence of time is evident both orchard-wide (varying cultivar maturity classes) and within each tree (successive epidemic phases from early to late). Time increases disease incidence through increasing inoculum loads both within each tree and as disease develops on successively later maturity classes across the orchard. This reduces the level of disease aggregation both via increasing disease incidence per tree and through an increase in the orchard-wide inoculum load providing more external sources of inoculum.

There were five out of 13 trees that had 10 or more blighted blossoms per tree, which allowed examination of spatial association of the pre-harvest fruit rot to blossom blight earlier in the season (table 2).With the exception of the smallest tree (O'Henry 127), all trees showed a significant positive association of pre-harvest fruit rot to blossom blight symptoms within the same canopy. This result is consistent with previous work showing that removing blighted blossoms reduced fruit rot incidence within an orchard (Dunegan and Goldsworthy 1948) and that blossom blight incidence within individual trees was related to latent fruit infections (Emery et al. 2000). Whether blossom blight provided a continuous source of inoculum through the fruit ripening phase to result in positive spatial association, or whether blossom blight led to latent infections that then served as the source of inoculum during the pre-harvest epidemic cannot be determined from this data.

Table 2. Spatial association patterns of pre-harvest brown rot, caused by *Monilinia fructicola*, in relation to blossom blight earlier in the season in 5 of 13 intensively mapped peach tree canopies

Cultivar and tree number[a]	Year	Pre-harvest fruit rot	Blighted blossoms	d_w[b]	P	Pattern of association
Redglobe 7	2009	87	30	**0.213**	0.000	Positive
O'Henry 26	2009	142	43	**0.101**	0.002	Positive
O'Henry 26	2010	88	10	**0.153**	0.010	Positive
O'Henry 26	2011	96	28	**0.174**	0.002	Positive
O'Henry 127	2009	38	22	0.125	0.297	n.s.

a. Arranged in order of earliest- to latest-maturing cultivar.

b. d_w represents the index of spatial disease association and is calculated based on the cumulative frequency distribution of nearest-neighbor distances among brown rot–affected fruit and blighted blossoms present in the same canopy earlier in the season. Significant positive values ($P \leq 0.05$, in bold) indicate positive spatial association.

Each tree was also analyzed for spatial association within the pre-harvest epidemic. Results revealed that most new fruit rot symptoms were either not significantly or were significantly negatively associated with previous fruit rot symptoms in the same tree canopy (table 3). Only two trees showed a significantly positive association between groups of fruit that became symptomatic within successive phases of the epidemic. There were no significant correlations or nonlinear relationships between the index of association and other variables such as number of fruit per tree or level of aggregation of diseased fruit in the previous phase (data not shown).

Table 3. Spatial association patterns among newly symptomatic fruit and those that were symptomatic in the previous period for pre-harvest brown rot, caused by *Monilinia fructicola*, in 13 intensively mapped peach tree canopies

Cultivar and tree number[a]	Year	Comparison	New fruit rot	Existing fruit rot	d_w[c]	P	Pattern of association
			Early-season cultivar				
Sureprince 79	2010	Mid vs. early	22	26	**−0.334**	0.004	Negative
		Late vs. mid	35	48	−0.186	0.116	n.s.
			Mid-season cultivars				
Redglobe 7	2009	Mid vs. early	37	26	0.149	0.337	n.s.
		Late vs. mid	24	63	0.211	0.143	n.s.
Contender 74	2010	Late vs. early	82	41	**−0.370**	0.000	Negative
Contender 75	2010	Mid vs. early	36	12	−0.116	0.628	n.s.
		Late vs. mid	11	48	0.122	0.979	n.s.
			Late-season cultivar				
O'Henry 26	2009	Mid vs. early	93	35	**−0.204**	0.000	Negative
		Late vs. mid	14	128	**−0.344**	0.030	Negative
O'Henry 26	2010	Mid vs. early	49	24	0.097	0.625	n.s.
		Late vs. mid	21	73	**−0.366**	0.003	Negative
O'Henry 26	2011	Mid vs. early	35	21	**−0.331**	0.000	Negative
		Late vs. mid	40	56	**−0.295**	0.002	Negative
O'Henry 127	2009	Late vs. early	13	25	−0.340	0.051	n.s.
Flameprince 45	2009	Late vs. early	47	122	−0.106	0.440	n.s.
Flameprince 45	2010	Early vs. GFR	64	10	**0.265**	0.001	Positive
		Mid vs. early	59	74	**0.191**	0.025	Positive
		Late vs. mid	22	133	**0.443**	0.000	Positive
Flameprince 87	2010	Mid vs. early	30	31	0.177	0.213	n.s.
		Late vs. mid	13	61	−0.290	0.136	n.s.
Flameprince 88	2010	Mid vs. early	16	30	**0.389**	0.005	Positive
		Late vs. mid	16	46	−0.221	0.281	n.s.
Flameprince 120	2009	Late vs. early	52	76	**−0.181**	0.032	Negative

a. Arranged in order of earliest- to latest-maturing cultivar.

b. Trees were monitored for disease at 1- to 4-day intervals during the pre-harvest period, and data were summarized for two, three, or four assessment periods for each tree. Spatial associations were calculated among the fruit that had become newly symptomatic during one period and those that were symptomatic in the previous period. In Flameprince 45 (2010), GFR represents fruit affected by green fruit rot that directly preceded the pre-harvest epidemic.

c. d_w represents the index of spatial disease association between the successive epidemic phases and is calculated based on the cumulative frequency distribution of nearest-neighbor distances among brown rot–affected fruit in one period and those that were symptomatic in the previous period. Significant positive values indicate positive spatial association, whereas significant negative values signify negative spatial association compared with the random simulation. Significant d_w values ($P \leq 0.05$) are in bold.

The lack of a positive spatial association among fruit that became symptomatic in a later phase of the epidemic with those that were symptomatic in the preceding phase in the same tree was unexpected in that it seemed reasonable to hypothesize that newly infected fruit would, on average, be closer to previously infected fruit than by random chance. Instead, eight of the 20 (= 40.0%) tree-epidemic phase comparison combinations showed significant negative associations, meaning that newly diseased fruit were on average farther away from previously diseased fruit than expected. One explanation for this may be related to the timescale over which associations were examined. For example, in some cases, each phase of the epidemic was delimited by periods with relatively fewer symptoms developing, with each wave of the epidemic considered part of the same epidemic phase. It is possible that an association between diseased fruit in the pre-harvest epidemic would be strongest during the time when conditions are conducive for disease (i.e., within each phase rather than between phases).

Another possible explanation for the negative association between phases of the epidemic may be that this is a reflection of the relatively greater importance of external sources of inoculum vs within-tree sources. This idea is supported by the fact that significant negative associations were more common (six out of 13 combinations = 46.2%) in late-season cultivars (where overall orchard-wide inoculum load would have been higher) than in early- and mid-season cultivars (two out of seven combinations = 28.6%). In addition to external inoculum load, another potential explanation for the lack of positive spatial associations among fruit becoming symptomatic within different epidemic phases may be that the pattern of fruit ripening may affect the timing of symptom development, such that uneven fruit ripening in different sectors of the canopy (Lewallen and Marini 2003) could lead to negative associations among newly developing brown rot symptoms.

Conclusions

We are aware of no previous studies that characterized the spatio-temporal within-canopy development of disease season-long across multiple years. High-resolution three-dimensional maps generated with a magnetic digitizer enabled characterization of disease aggregation and association patterns within each of the 13 intensively monitored trees. In general, this approach to canopy mapping and spatial analysis should be applicable to a wide range of studies in plant pathology, pest management, and canopy ecology in trees with complex architecture. For pre-harvest brown rot of peach, our analyses supported some commonly held epidemiological concepts, e.g., that aggregation among symptomatic individuals decreases as disease incidence increases, and that fruit rot symptoms are positively associated with the locations of blossom blight earlier in the season. However, the analyses also revealed complex interactions between time, cultivar maturity season, within-tree epidemic phase, disease incidence, and disease aggregation that could not have been predicted a priori. Finally, the analyses also produced some unexpected results, particularly the lack of a positive spatial association among fruit that became symptomatic in a later phase of the epidemic with those that were symptomatic in the preceding phase in the same tree, leading to the formulation of testable hypotheses about the impact of uneven fruit ripening patterns within the tree on disease spread. Ultimately, the high complexity of tree canopies

is evidenced by this outcome, whereby factors such as microclimatic variation, host physiology, and biotic influences (bird or insect damage) may play an important role in shaping disease aggregation and association patterns. Further interpretation of the spatial patterns observed in this study will be possible through population genetics analyses of pathogen isolates obtained from each symptomatic fruit in select trees in this study (Everhart 2012).

Acknowledgments – We thank Amy Savelle, Sara Thomas, and Lucky Mehra for their assistance in digitizing tree canopies. Funded in part by grant no. 2009-34103-19818 from the USDA Southern Region IPM Program. Additional financial support provided by the American Phytopathological Society's Tarleton Fellowship, a Sigma Xi Grant-in-Aid of Research, and a University of Georgia Dissertation Completion Award to S.E.E.

References

Batzer, J. C., Gleason, M. L., Taylor, S. E., Koehler, K. J., & Monteiro, J. E. B. A. (2008). Spatial heterogeneity of leaf wetness duration in apple trees and its influence on performance of a warning system for sooty blotch and flyspeck. *Plant Disease*, 92, 164–170.

Coomes, D., Rees, M., & Turnbull, L. (1999). Identifying aggregation and association in fully mapped spatial data. *Ecology*, 80, 554–565.

Dunegan, J. C., & Goldsworthy, M. C. (1948). The control of blossom blight and its relation to brown rot of Red Bird peaches at harvest. *Plant Disease Reporter*, 32, 136–137.

Emery, K. M., Michailides, T. J., & Scherm, H. (2000). Incidence of latent infection of immature peach fruit by *Monilinia fructicola* and relationship to brown rot in Georgia. *Plant Disease*, 84, 853–857.

Everhart, S. E. (2012). Spatial Pattern of Brown Rot Symptoms and Fine-Scale Genetic Structure of *Monilinia fructicola* within Stone Fruit Tree Canopies. Athens, GA: Ph.D. dissertation, University of Georgia.

Everhart, S. E., Askew, A., Seymour, L., Holb, I. J., & Scherm, H. (2011). Characterization of three-dimensional spatial aggregation and association patterns of brown rot symptoms within intensively mapped sour cherry trees. *Annals of Botany*, 108, 1195–1202.

Everhart, S. E., Askew, A., Seymour, L., Glenn, T. C., & Scherm, H. (2012). Spatial patterns of brown rot epidemics and development of microsatellite markers for analyzing fine-scale genetic structure of *Monilinia fructicola* populations within peach tree canopies. *Plant Health Progress, Online*. doi: 10.1094/PHP-2012-0723-04-RS

Holb, I. J., & Scherm, H. (2007). Temporal dynamics of brown rot in different apple management systems and importance of dropped fruit for disease development. *Phytopathology*, 97, 1104–1111.

Horton, D., Brannen, P., Bellinger, B., Lockwood, D., & Ritchie, D. (2011). Southeastern peach, nectarine, and plum pest management and culture guide. Athens: University of Georgia Cooperative Extension Service.

Jeger, M. J. (1999). Improved understanding of dispersal in crop pest and disease management: current status and future directions. *Agricultural and Forest Meteorology*, 97, 331–349.

Kable, P. (1969). Brown rot of stone fruits on the Murrumbidgee Irrigation Areas. I. Aetiology of the disease in canning peaches. *Australian Journal of Agricultural Research*, 20, 301–316.

Lewallen, K. S., & Marini, R. P. (2003). Relationship between flesh firmness and ground color in peach as influenced by light and canopy position. *Journal of the American Society for Horticultural Science*, 128, 163–170.

Madden, L. V., Hughes, G., van den Bosch, F. (2007). Spatial aspects of epidemics – III: Patterns of plant disease. Pages 235–278 in: *The Study of Plant Disease Epidemics*. St. Paul, MN: American Phytopathological Society.

Moslonka-Lefebvre, M., Finley, A., Dorigatti, I., Dehnen-Schmutz, K., Harwood, T., Jeger, M. J., Xu, X., Holdenrieder, O., & Pautasso, M. (2010). Networks in plant epidemiology: from genes to landscapes, countries, and continents. *Phytopathology*, 101, 392–403.

Pethybridge, S. J., Hay, F. S., & Gent, D. H. (2010). Characterization of the spatiotemporal attributes of *Sclerotinia* flower blight epidemics in a perennial pyrethrum pathosystem. *Plant Disease*, 94, 1305–1313.

Plantegenest, M., Le May, C., & Fabre, F. (2007). Landscape epidemiology of plant diseases. *Journal of the Royal Society, Interface*, 4, 963–972.

Sinoquet, H., Rivet, P., & Godin, C. (1997). Assessment of the three-dimensional architecture of walnut trees using digitising. *Silva Fennica*, 31, 265–273.

Smith, F. D., & MacHardy, W. E. (1984). The retention and redistribution of captan on apple foliage. *Phytopathology*, 74, 894–899.

Spósito, M. B., Amorim, L., Bassanezi, R. B., Filho, A. B., & Hau, B. (2008). Spatial pattern of black spot incidence within citrus trees related to disease severity and pathogen dispersal. *Plant Pathology*, 57, 103–108.

Vereijssen, J., Schneider, J., Stein, A., & Jeger, M. (2006). Spatial pattern of Cercospora leaf spot of sugar beet in fields in long- and recently-established areas. *European Journal of Plant Pathology*, 116, 187–198.

Vereijssen, J., Schneider, J. H. M., & Jeger, M. J. (2007). Epidemiology of Cercospora leaf spot on sugar beet: modeling disease dynamics within and between individual plants. *Phytopathology*, 97, 1550–1557.

Waggoner, P. E., & Aylor, D. E. (2000). Epidemiology: a science of patterns. *Annual Review of Phytopathology*, 38, 71–94.